pp 244–255. © The Author(s), 2020. Published by Cambridge University Press on behalf of Royal Aeronautical Society
doi:10.1017/aer.2020.51

The vibration suppression of solar panel based on smart structure

G. Ma
qiuyexinjun@xatu.edu.cn
School of Mechatronic Engineering
Xi'an Technological University
Xi'an
China

State Key Laboratory for Strength and Vibration of Mechanical Structures
School of Aerospace
Xi'an Jiaotong University
Xi'an
China

M. Xu
State Key Laboratory for Strength and Vibration of Mechanical Structures
School of Aerospace
Xi'an Jiaotong University
Xi'an
China

J. Tian
School of Mechatronic Engineering
Xi'an Technological University
Xi'an
China

X. Kan
School of Mechanical and Precision Instrument Engineering
Xi'an University of Technology
Xi'an
China

ABSTRACT

This paper provides a solution to the active vibration control of a microsatellite with two solar panels. At first, the microsatellite is processed as a finite element model containing a rigid body and two flexible bodies, according to the principles of mechanics, and that the

Received 19 December 2019; revised 19 May 2020; accepted 20 May 2020.

dynamic characteristics are solved by modal analysis. Secondly, the equation involving vibration control is established according to the finite element calculation results. There are several actuators composed of macro fibre composite on the two solar panels for outputting control force. Furthermore, the control voltage for driving actuator is calculated by using fuzzy algorithm. It is clear that the smart structure consists of the flexible bodies and actuators. Finally, the closed-loop control simulation for suppressing harmful vibration is established. The simulation results illustrate that the responses to the external excitation are decreased significantly after adopting fuzzy control.

Keywords: Microsatellite; AVC; smart structure; MFC

NOMENCLATURE

$\boldsymbol{E}$	Young's modulus
$\boldsymbol{M_n}$	regularization mass matrix
$\boldsymbol{K_n}$	stiffness matrix
$\boldsymbol{C_n}$	Rayleigh damping matrix
$\boldsymbol{I_n}$	unit matrix
q_n	time-domain response
f_a	unit force
V(t)	voltage
k_e	quantization factor
k_{ec}	quantization factor
k_u	perameter factor
$u(x'_k)$	membership value
x'_k	fuzzy data
x'	output signal
$\boldsymbol{x}$	state vector
$\boldsymbol{f}$	force vector
$\boldsymbol{A}$	system matrix
$\boldsymbol{B}$	input matrix
F_e	exiataion force
F_a	control force
M_a	unit bending moment
f_n(Hz)	natural frequency

Greek Symbol

α_T	coefficient of thermal expansion
α	perameter
β	perameter

https://doi.org/10.1017/aer.2020.51 Published online by Cambridge University Press

ζ	damping ratio
Ω_n(rad)	natural frequency
ρ	density
ν	Poisson's ratio

1.0 INTRODUCTION

In general, a microsatellite is composed of a rigid body and several flexible appendages, such as solar panel, antenna and so on, and these appendages are flexible with the characteristics of light weight, great flexibility and weak damping, which induce low frequency vibration. When the external excitation affects the low-frequency vibration of flexible structure, the dynamic response becomes more complex considering the typical characteristics. For example, if the microsatellite is subjected to the transient excitation and steady-state excitation, the dynamic response will produce large amplitude and slow attenuation process. Especially, once the disturbance frequency is close to the fundamental frequency of a flexible structure, the resonance phenomenon occurs immediately. This phenomenon must give rise to seriously dynamic response impacting on the performances of microsatellite such as stability, reliability, accuracy and so on. Because most of the microsatellites are used for the data transmission of space and ground, a small problem causes a serious accident accordingly. What is more, the microsatellite may be scrapped under certain circumstances. As viewed from these problems, in order to suppress the vibration of flexible structures, smart material is applied to design smart structure to establish the active vibration control (AVC) system, which is closed-loop control system[1,2]. It is generally true that the key technologies are control algorithms, sensors and actuators.

In recent years, different control algorithms have been discussed. For example, Li[3] designed a piezoelectric adaptive truss using the linear quadratic Gaussian control. Luo[4] used PD control for vibration suppression of a hoop truss structure based on a novel piezoelectric bending actuator. Mystkowski[5] adopted robust control for a three-dimensional flexible bar using PZT actuators. Zhao[6] applied a new numerical method to investigate the vibration control of an axially translating robot arm using displacement and velocity control law. Kim[7] presented the vibration control of a trailed two-wheeled implement using sliding mode control. Moreover, based on global analytical modes, Liu[8] developed a rigid-flexible coupling dynamic model for spacecraft with solar panel. This model enables the convenient and precise calculation of natural characteristics and includes an attitude control law for suppressing vibration simultaneously. Besides, there are other control algorithms for establishing the vibration control systems[9,10]. Among these control algorithms, PD control is a kind of linear feedback control algorithm, and it is easy to design and operate. However, fuzzy control is a kind of logic control algorithm, and it is suitable for flexible objects like solar panel.

Because the sensors and actuators are designed by various piezoelectric materials, they are widely applied. But the stiffness of ordinary piezoelectric material is relatively large. For example, some actuators fabricated from PZT have high sensitivity, but they have great stiffness and brittleness. Therefore, considering that the solar panel in the satellite is easily vibrated to give rise to large deformation, scholars' studies may be more reasonable if the structure applies flexible sensor and actuator. There are highly sensitive and flexible strain gauges, but complicated bridges need to be measured. In addition, strain gauges are also susceptible to temperature. Compared with traditional materials, macro fibre composite (MFC)

https://doi.org/10.1017/aer.2020.51 Published online by Cambridge University Press

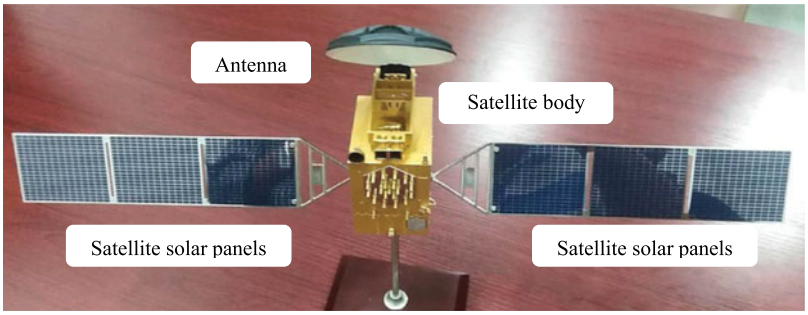

Figure 1. The satellite model.

is a developed smart material, and more flexible. The MFC has been widely applied in various situations[11,12,13]. This new material is originally developed as a means of overcoming many of the practical difficulties associated with using monolithic piezoelectric actuators in structural control applications[14]. Sohn[15] also observed that this material has excellent sensing performance in measuring dynamic response and monitoring structural vibration. In a word, this new piezoelectric material is suitable for designing sensor and actuator. For example, Steiger[12] proposed MFC as actuator by means of negative capacitance shunted circuit. Zhang[13] used MFC as actuator for suppressing plate-like solar panels. If the sensors and actuators are all flexible, the AVC will be widely used in aerospace field.

This paper proposes a vibration suppression method of a microsatellite with two solar panels based on smart structure by using of MFC sensor and actuator. The remaining parts of the paper are organised as follows. In Section 2, the mode analysis of a microsatellite is investigated to obtain the vibration characteristics, and the state space equation is established with consideration of fuzzy algorithm. In Section 3, a simulation program is presented to refer to control principle, and the dynamic responses to three excitations are significantly decreased after applying the fuzzy control.

2.0 MODE AND THEORETICAL ANALYSIS

2.1 Mode analysis

Here is a microsatellite that consists of a rigid body, two solar panels, an antenna and other appendages, as shown in Fig. 1. Because vibration characteristics are the basis of the AVC, the frequencies, modes and other characteristics of microsatellite need to be calculated. According to the mechanics theory, a satellite system is modeling as a rigid-flexible coupling multi-body system. When the main flexible body is solar panel, only the characteristics of solar panel is analysed in the mode analysis. MSC Patran is used to establish a three-dimensional finite element model on account of the parameters in Table 1. This model consists of two solar panels and several flexible beams. The two solar panels with MFC patches constitute two smart structures, where the sensors and actuators are flexible.

The model contains 354 nodes, 20 CBAR elements, 140 CQUAD4 elements and 6 MFC elements. Then MSC Nastran is used to solve the natural frequencies and modes using Lanczos method. Generally, a flexible structure has complex vibration modes. With consideration of low-frequency vibration, there are the first four order modes selected as shown in Fig. 2.

https://doi.org/10.1017/aer.2020.51 Published online by Cambridge University Press

Table 1
The satellite parameters

Structure	Thickness (mm)	Length (mm)	Width (mm)	E (GPa)	ν	α_T	ρ (kg/m^3)
Solar panel	1	500	200	130	0.2	2.6e-6	2300
MFC	0.3	50	28.57	30GPa	0.31	15e-6	5440
Rigid body	250	250	250	70GPa	0.3	Normal	2700
Flexible beam	length=141.4, side length=10			70GPa	0.3	Normal	2700

Table 2
The microsatellite frequencies

Case	Mode 1, f_1	Mode 2, f_2	Mode 3, f_3	Mode 4, f_4
No actuator	3.451Hz	24.575Hz	25.097Hz	42.667Hz
With actuator	3.452Hz	24.537Hz	25.096Hz	42.587Hz
Error	0.02%	0.15%	0%	0.18%

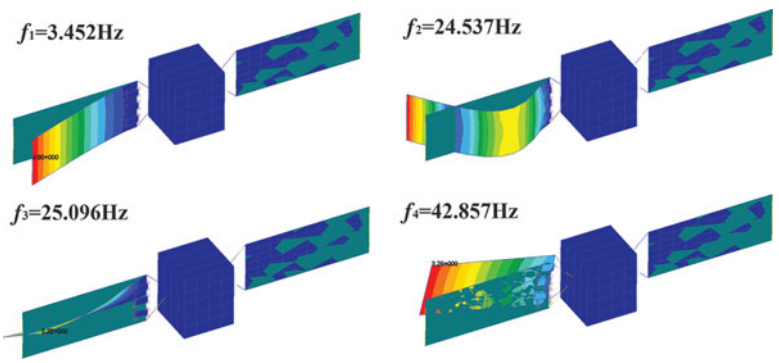

Figure 2. The first four order modes of satellite.

It is found that the first and second order modes are the deformation of solar panel, similar to a bending beam. What is more, the first order natural frequency is 3.452Hz belonging to low frequency, and these patches have almost no effect on the frequency as shown in Table 2.

2.2 The vibration control theoretical analysis

It is usually that the AVC is suitable to suppress low-frequency vibration. Because the vibration of the solar panel is just low-frequency vibration, the AVC is used to suppress the

https://doi.org/10.1017/aer.2020.51 Published online by Cambridge University Press

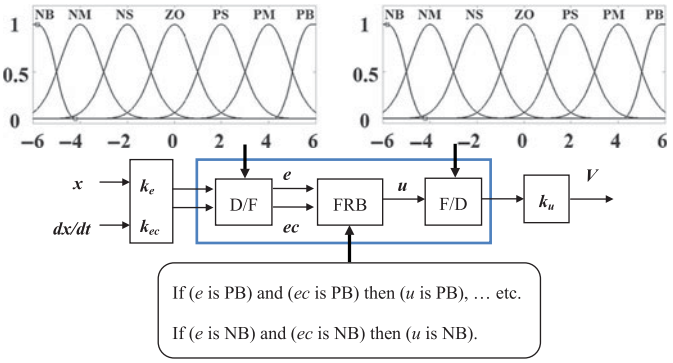

Figure 3. Fuzzy controller.

vibration of the solar panel. This research object is a multi-degree of freedom structure, and the vibration equation of closed-loop control system is

$$\mathrm{M}_n\ddot{q}_n + C_n\dot{q}_n + K_n q_n = \phi_n F_e + \phi_n F_a, \quad \ldots(1)$$

where $\boldsymbol{M_n}$, $\boldsymbol{K_n}$ and are the regularization mass, stiffness matrices respectively,

$$M_n = I_n, K_n = 2\pi \cdot diag\left[\omega_n\right], \quad \ldots(2)$$

where $\omega_n = 2\pi f_n$, $\boldsymbol{C_n}$ is reflected as the Rayleigh damping matrix,

$$C_n = \alpha M_n + \beta K_n, \quad \ldots(3)$$

where the two perameters α, β are constructed by Equation (3) containing natural frequency ω_n and damping ratio ζ,

$$a = \left[\frac{1}{\omega_1}\ \omega_1; \frac{1}{\omega_2}\ \omega_2\right]; b = 2\begin{bmatrix}\zeta\\ \zeta\end{bmatrix}; \alpha = a^{-1}b\,[1]; \beta = a^{-1}b\,[2] \quad \ldots(4)$$

These characteristic parameters have been calculated by the finite element analysis above. Besides, q_n is time-domain response representing output, ϕ_n is spatial displacement function, F_e is disturbance excitation, F_a is control force generated by MFC actuator. In the case of negative feedback signal adopting fuzzy algorithm, the control force and control voltage is,

$$F_a = f_a V\,(t)\,,\ V\,(t) = F_u\left[-k_e q, -k_{ec}\dot{q}\right] k_u, \quad \ldots(5)$$

where f_a is unit force, $V(t)$ is control voltage, k_e, k_{ec} and k_u are the parameters, respectively.

Figure 3 shows the fuzzy controller where the input signal is divided into two signals x and dx/dt, and the two signals are multiplied by the quantisation factors k_e and k_{ec} to quantise the signals. Then the signals are taken for fuzzy processing to output definite fuzzy data.

The fuzzy processing contains three steps such as fuzzification (D/F), fuzzy rule base (FRB) and inverse operation of fuzzification (F/D). At the beginning of fuzzy processing, $x\,k_e$ and $(dx/dt)\,k_{ec}$ are converted into fuzzy field through the fuzzification, where the membership function is ec[-6 6] and e[-6 6]. Secondly, the fuzzy rule base adopts Mamdani-type

https://doi.org/10.1017/aer.2020.51 Published online by Cambridge University Press

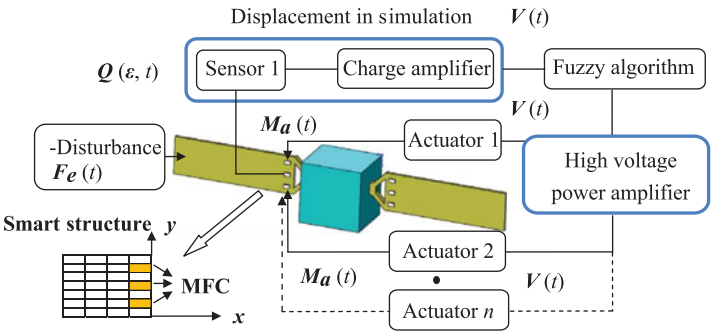

Figure 4. Control principle.

logic ruler to deal with the two-dimensional data. Thirdly, the data after operating in the previous step are determined through the F/D process, where the membership function is u[-6 6]. Finally, if the F/D process adopts gravity center method, the output signal x' multiplied by ku will be control signal.

$$x' = \sum_{k=1}^{n} u(x'_k) \cdot x'_k \Big/ \sum_{k=1}^{n} u(x'_k), \qquad \ldots (6)$$

where $u(x'_k)$ is membership value, x'_k is fuzzy data.

Substitute Equations (2)-(5) into Equation (1), and reduce the degrees of freedom by means of mode truncation method; the vibration equation can be reduced to a state space equation Equation (7) describing the transfer of input and output signals. Then the solution is just the response.

$$\dot{x} = Ax + Bf, \qquad \ldots (7)$$

where $\boldsymbol{x}$ is state vector, $\boldsymbol{A}$ is system matrix, $\boldsymbol{B}$ is input matrix, and $\boldsymbol{f}$ is force vector, respectively.

$$x = \begin{Bmatrix} \dot{q} \\ q \end{Bmatrix}; A = -B \begin{bmatrix} -M_n & 0 \\ 0 & K_n \end{bmatrix};$$
$$B = \begin{bmatrix} 0 & M_n \\ M_n & C_n \end{bmatrix}^{-1}; f = \begin{bmatrix} 0 & \phi_n F_e + \phi_n f_a F_u \left[-k_e q_n, -k_{ec} \dot{q}_n\right] k_u \end{bmatrix} \qquad \ldots (8)$$

3.0 THE ACTIVE VIBRATION CONTROL SIMULATION

3.1 The control method

The control system consists of sensor, charge amplifier, control algorithm, actuator, high-voltage power amplifier and other devices in the experiment are shown in Fig. 4. In this section, Matlab/Simulink is applied to set up the closed-loop control simulation for the first order mode of solar panel as shown in Fig. 5. Although the MFC sensor outputs strain in

https://doi.org/10.1017/aer.2020.51 Published online by Cambridge University Press

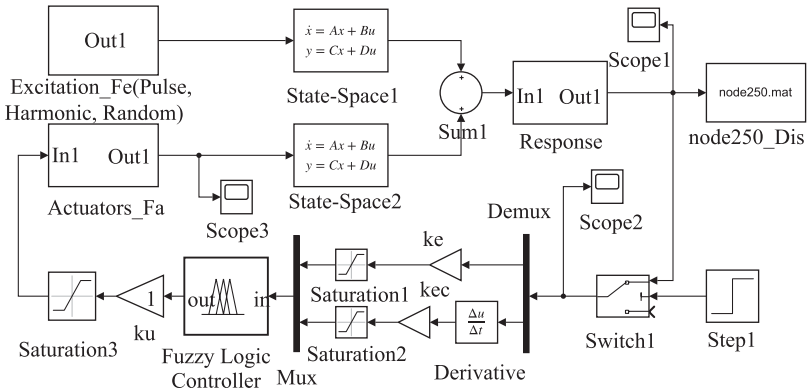

Figure 5. Simulation program.

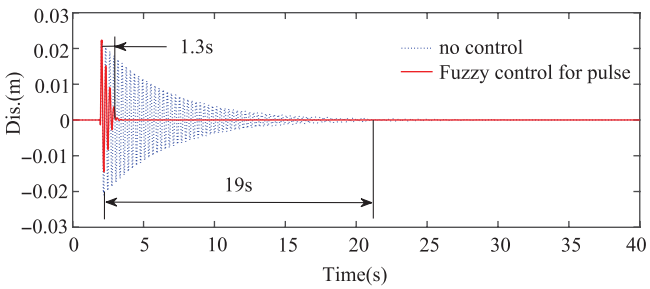

Figure 6. Fuzzy control for pulse excitation.

practice, the simulation adopts displacement sensor (Out1) instead of strain sensor because of the linear correlation between strain and displacement. Furthermore, the excitation signal F_e is pulse, harmonic or random signals, respectively. The solution to the state space equation is just as response and feedback signal that is calculated by fuzzy algorithm to produce control signal. Meanwhile, the MFC actuators convert the control signal into force $F_a(M_a)$ in order to suppress the vibration, where the unit-bending moment M_a is set to 2 Nm/100V.

3.2 The simulation result

Figure 6 shows the response of node 250 on the finite element model after pulse excitation. As the amplitude droppers to 5% of the peak, the attenuation time lasts 19s. When the fuzzy control adds in the response, the attenuation time is 1.3s. As a result, the attenuation ratio is 93.15%. It is thus clear that the attenuation time is greatly shortened.

Figure 7 shows the sinusoidal excitation and random excitation, and the mean and variance of random excitation is 0 and 1, respectively. Figures 8 and 9 show the response of node 250 after fuzzy control. At the beginning, there is only the excitation, but the control force begins to affect the solar panel after 20s.

https://doi.org/10.1017/aer.2020.51 Published online by Cambridge University Press

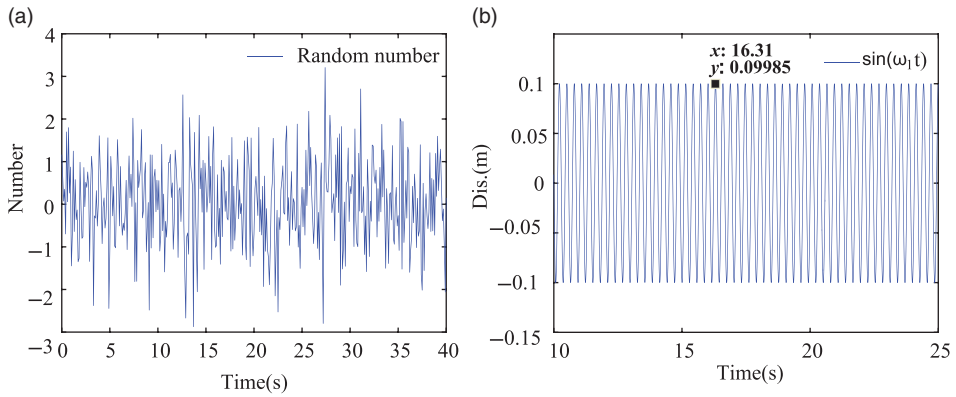

Figure 7. Harmonic excitation and random excitation.

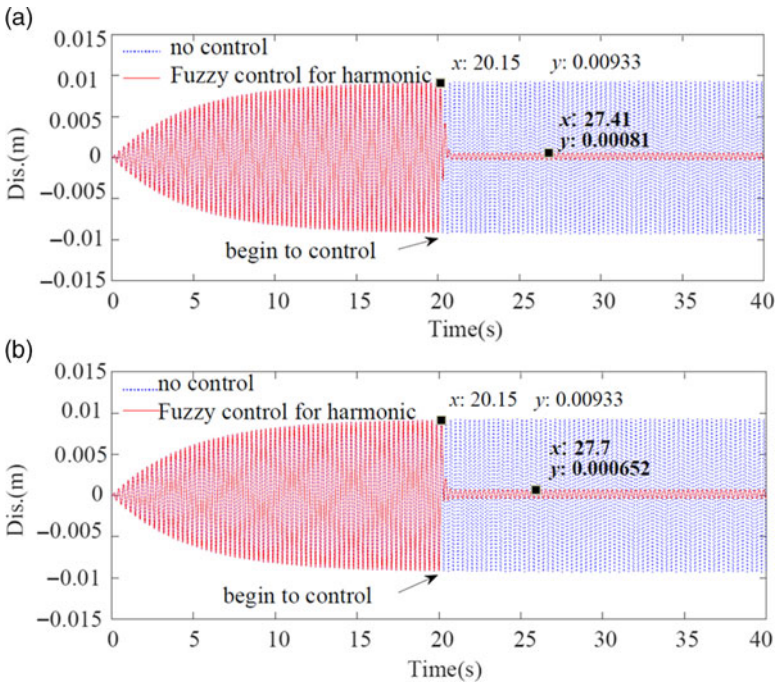

Figure 8. (a) Fuzzy control for harmonic excitation. (b) Fuzzy control for harmonic excitation.

As is shown in the Figs. 8 and 9, it can be seen that the curves of steady-state vibration and random vibration are obviously decreased. For example, Fig. 8(a) shows the response amplitudes are 0.00933 and 0.00081m before fuzzy control and after fuzzy control, respectively, and the corresponding amplitude suppression rate is 91.32%. When the response amplitude after fuzzy control is 0.000652m shown in Fig. 8(b), the amplitude suppression rate is 93.01%.

https://doi.org/10.1017/aer.2020.51 Published online by Cambridge University Press

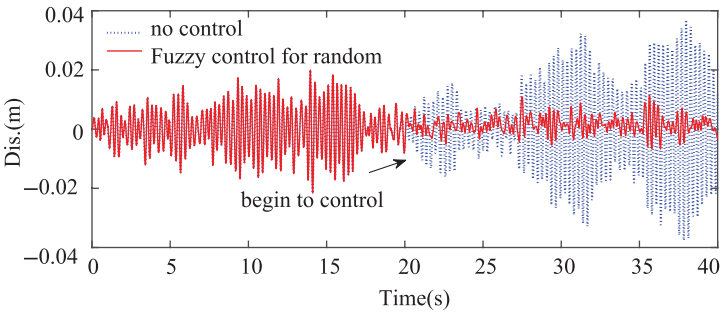

Figure 9. Fuzzy control for random excitation.

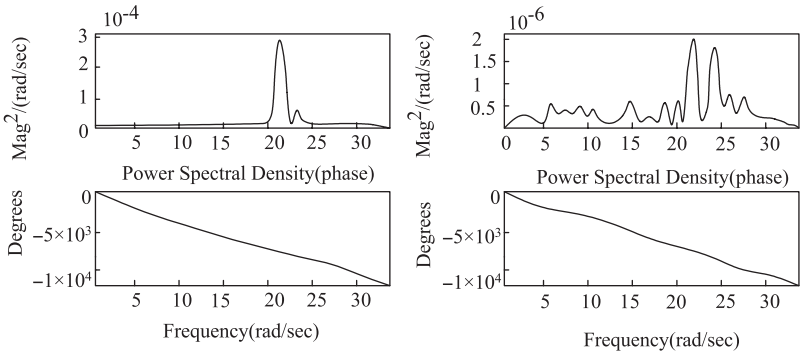

Figure 10. PSD before control and after control.

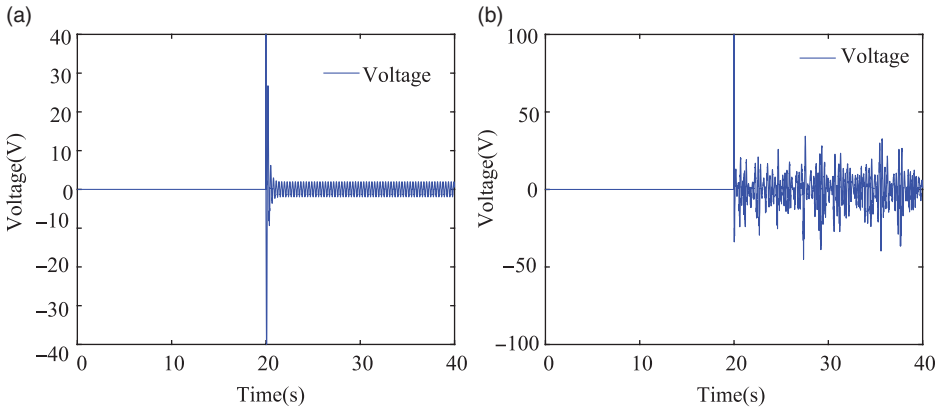

Figure 11. Control voltage.

As for the random vibration, the power spectral density reduces to 0.7% shown in Fig. 10. Fig. 11 shows the control voltages when the excitations are harmonic and random excitations respectively. Table 3 shows the parameters of fuzzy controller and control results.

https://doi.org/10.1017/aer.2020.51 Published online by Cambridge University Press

Table 3
The suppression result

Excitation	Pulse	Harmonic	Random	Another Harmonic
Parameters	same parameters: $k_e = 3$, $k_{ec} = -3$, $k_u = 1$			$k_e = 2$, $k_{ec} = -2$, $k_u = 2$
Result	attenuation rate	suppression rate	PSD	suppression rate
Ratio %	93.15%	91.32%	0.7%	93.01%

4.0 CONCLUSION

This paper provides a vibration suppression method of a microsatellite consisting of two solar panels and several MFC patches. According to the present calculation and simulation, the following main conclusions are obtained. In the mode analysis, the MFC patches have little effect on the natural frequencies, and the first four order modes show the deformation of solar panel. What is more, the first frequency is low, and the first order mode is bending mode. In the simulation, the external excitation can result in significant response. However, it is obvious that the response can be suppressed dramatically by the actuators. The figures and tables are presented to illustrate the control results after adopting fuzzy algorithm. It is found that the amplitude inhibition percentages are all more than 90%. Moreover, the power spectral density falls by two orders of magnitude. Consequently, based on smart structure embodying flexible sensor, actuator and fuzzy algorithm, the AVC is effective for solar panel vibration suppression.

ACKNOWLEDGMENTS

This work is supported by the State Key Laboratory for Strength and Vibration of Mechanical Structures (Grant no. SV2020-KF-01), and the Basic Research Plan of Natural Science in Shannxi Province (No.2018JM5099).

REFERENCES

1. AN, Z.Y., XU, M.L., LUO, Y.J., and WU, C.S. Active vibration control for a large annular flexible structure via a macro-fiber composite strain sensor and voice coil actuator, *Int J Appl Mech*, 2015, **7**, (4), 1550066.
2. MA, G.L., GAO, B., XU, M.L., and FENG, B. Active suspension method and active vibration control of a hoop truss structure, *AIAA J*, 2018, **56**, (4), pp 1689–1695.
3. LI, W.P., and HUANG, H. Integrated optimization of actuator placement and vibration control for PZT adaptive trusses, *J Sound Vibr*, 2013, **332**, (1), pp 17–32.
4. LUO, Y.J., XU, M.L., YAN, B., and ZHANG, X.N. PD control for vibration attenuation in Hoop truss structure based on a novel piezoelectric bending actuator, *J Sound Vibr*, 2015, **339**, pp 11–24.
5. MYSTKOWSKI, A. and KOSZEWNIK, A.P. Mu-Synthesis robust control of 3D bar structure vibration using piezo-stack actuators, *Mech Syst Sig Process*, 2016, **78**, pp 18–27.
6. ZHAO, L., and HU, Z.D. Active vibration control of an axially translating robot arm with rotating-prismatic joint using self-sensing actuator, *Shock Vibr*, 2015, Article ID 964139.
7. KIM, H.J. Investigation of active vibration control system for trailed two-wheeled implements, *Proc Inst Mech Eng Part C J Mech Eng Sci*, 2012, **226**, (1), pp 55–65.

https://doi.org/10.1017/aer.2020.51 Published online by Cambridge University Press

8. LIU, L., CAO, D.Q. and WEI, J. Rigid-flexible coupling dynamic modeling and vibration control for flexible spacecraft based on its global analytical modes, *Sci China Tech Sci*, 2019, **62**, (4), pp 608–618.
9. MOTTA, V. and QUARANTA, G. A comparative assessment of vibration control capabilities of a L-shaped Gurney flap, *Aeronaut J*, 2016, **120**, (1233), pp. 1812–1831.
10. BRILLANTE, C., MORANDINI M. and MANTEGAZZA, P. Periodic controllers for vibration reduction using actively twisted blades, *Aeronaut J*, 2016, **120**, (1233), pp. 1763–1784.
11. RO, J.J., CHIEN, C.C., WEI, T.Y. and SUN, S.J. Flexural vibration control of the circular handlebars of a bicycle by using MFC actuators, *J Vibr Control*, 2007, **13**, (7), pp 969–987.
12. STEIGER, K. and MOKRY, P. Finite element analysis of the macro fiber composite actuator: macroscopic elastic and piezoelectric properties and active control thereof by means of negative capacitance shunt circuit, *Smart Mater Struct*, 2015, **24**, (2), 025026.
13. ZHANG, C.L., ZHANG, X.N., XU, M.L. and LUO, Y.J. Active control of honeycomb sandwich plate using MFC piezoelectric actuators, *Int J Appl Electromagnet Mech*, 2014, **45**, (1), pp 83–91.
14. BENT, A. Active fiber composite material systems for structural control applications, Proceedings, SPIE's 6th International Symposium on Smart Structures and Materials, Newport Beach, CA, March 1–5 1999, SPIE 3674.
15. SOHN, J.W., JEON, J. and CHOI, S.B. An investigation on dynamic signals of MFC and PVDF sensors: Experimental work, *Adv Mech Eng*, 2015, **5**, 420345.

https://doi.org/10.1017/aer.2020.51 Published online by Cambridge University Press